quency if $\omega\tau \gg 1$. If $\omega\tau$ is not much greater than one, then one expects a variation of σ_1^r/σ_1^0 with wavelength. Interband effects also will produce a variation of σ_1^r/σ_1^0 with wavelength. For Ag over the range measured, $\omega\tau \gg 1$, while for Al one expects $\omega\tau$ effects to start producing a variation in σ_1^r/σ_1^0 near the long-wavelength end of the measured region.

The only previous experimental measurements to compare the measurements with are those of Majorana. Majorana used a tungsten light source and a Na photocathode. This combination has a peak sensitivity centered around 4500 Å. Table I shows the Majorana values χ, which are in reasonable agreement with our measurements in the vicinity of 4500 Å.

VI. CONCLUSIONS

In this paper the first detailed study of the PRFE in aluminum and silver has been presented. It has been found possible to measure the effect with an accuracy of a few percent. Arguments have been presented indicating, at least for Al, that the property measured is characteristic of the bulk. The determination of the real and imaginary parts of σ_1 for Al has not been possible because the optical constants are not known with sufficient accuracy. For Ag the results are in reasonable agreement with the intraband theory.

ACKNOWLEDGMENTS

The authors are pleased to acknowledge the aid of A. J. McAlister in taking much of the data reported in this paper. We also wish to thank Dr. S. K. Ghosh for preparing one of the samples and A. Bhatnagar for measuring some of the optical constants. One of us (J. M.) is grateful for a National Science Foundation cooperative fellowship for the period during which the major portion of this work was completed.

PHYSICAL REVIEW VOLUME 135, NUMBER 5A 31 AUGUST 1964

High-Temperature Susceptibility of Heisenberg Ferromagnets Having First- and Second-Neighbor Interactions*

PETER J. WOJTOWICZ
RCA Laboratories, Princeton, New Jersey

AND

R. I. JOSEPH
Raytheon Research Division, Waltham, Massachusetts

(Received 5 March 1964)

Exact power-series expansion of the high-temperature magnetic susceptibility of the nearest-neighbor Heisenberg ferromagnets have been provided by Rushbrooke and Wood. This paper describes the derivation of high-temperature susceptibility series for Heisenberg ferromagnets having both first- and second-neighbor exchange. The calculation is accomplished by extending the general diagrammatic technique developed by Rushbrooke and Wood to include the second-neighbor interaction. All mixed coefficients for terms through the fourth power of the inverse temperature have been computed for arbitrary spin and general lattice structure. The series expansions have been applied to the susceptibility of gadolinium in order to determine the quality of information which can be obtained from experimental data. It is found that the susceptibility is not quite sensitive enough to be able to specify the values of both the first- and second-neighbor exchange constants. It is shown, however, that the theory is capable of providing one definite relationship between the values of the two constants. The determination of unique values for the constants then requires the analysis of additional experimental data. The value of the Curie constant is uniquely specified.

I. INTRODUCTION

THE theory of the high-temperature susceptibility of the Heisenberg model ferromagnets has been advanced to a high degree of approximation through the extensive development of the exact power-series expansion method of Kramers and Opechowski[1] by Rushbrooke and Wood[2] (their paper shall henceforth be denoted by R-W). With this technique the susceptibility is expressed as a Taylor series in ascending powers of the reciprocal temperature. The coefficients of the series are then evaluated using a systematic and powerful diagrammatic analysis. All coefficients through the sixth-power term have been computed in R-W for general spin and arbitrary lattices. These six coefficients have been further generalized by Morgan and Rushbrooke[3] to include the concentration dependence in ferromagnets containing random admixtures of nonmagnetic elements.

* This research was independently supported by the RCA Laboratories and the Raytheon Research Division.

[1] W. Opechowski, Physica 4, 181 (1937); 6, 1112 (1938).

[2] G. S. Rushbrooke and P. J. Wood, Mol. Phys. 1, 257 (1958); denoted by R-W in the text.

[3] D. J. Morgan and G. S. Rushbrooke, Mol. Phys. 4, 291 (1961).

At this stage of development the applicability of the susceptibility series is still somewhat limited, however. The principal restricting feature of the current theory is the assumption that exchange interactions exist only between nearest-neighboring pairs of spins. In a wide variety of materials it is quite likely that interactions between second- and higher-order neighbor pairs will have magnitudes which are too large to be neglected. Sáenz[4] has included arbitrarily distant pair exchange interactions in the series expansion method but has only applied these considerations explicitly to the problem of magnetic scattering of neutrons.[5] In the present article we attempt to increase the utility of the susceptibility expansions by extending the results in R-W to include the effects of second-nearest-neighbor interactions.

Section II contains the formal statistical mechanical derivation of the susceptibility expansions based on a Heisenberg Hamiltonian containing both first- and second-neighbor interactions.

Section III describes the calculation of the mixed terms using an extension of the diagram method described in R-W. All mixed coefficients through the fourth-power term in the inverse temperature have been obtained for general spin and arbitrary lattices. In Sec. IV we consider the application of the enlarged susceptibility expressions to the determination of the first- and second-neighbor exchange constants of ferromagnetic gadolinium metal.

II. FORMAL STATISTICAL MECHANICS

The derivation of the susceptibility series follows very closely that given in R-W. In this article we shall therefore concentrate mainly on those new points brought about by the addition of second-neighbor interactions. The physical system of interest consists of a lattice of N sites containing atoms of spin S and gyromagnetic ratio g. Each atom will have z nearest-neighbor atoms and y second-neighbor atoms. The Hamiltonian of this system in the presence of an external magnetic field H_z is assumed to be

$$\begin{aligned}&\mathcal{H}=-2J_1\mathbf{P}-2J_2\mathbf{R}-g\mu H_z\mathbf{Q}\,,\\&\mathbf{P}=\textstyle\sum_{ij}\mathbf{S}_i\cdot\mathbf{S}_j\,,\\&\mathbf{R}=\textstyle\sum_{kl}\mathbf{S}_k\cdot\mathbf{S}_l\,,\\&\mathbf{Q}=\textstyle\sum_m\mathbf{S}_{mz}\,,\end{aligned}\tag{1}$$

where J_1 and J_2 are the magnitudes of the first- and second-neighbor exchange interactions, respectively, and where μ is the Bohr magneton. $\mathbf{P}$ and $\mathbf{R}$ are the sum of Heisenberg exchange operators for all first- and second-neighbor pairs, respectively, while $-g\mu H_z\mathbf{Q}$ is the Zeeman energy operator for the entire lattice. The operator $\mathbf{Q}$ commutes with both $\mathbf{P}$ and $\mathbf{R}$, but $\mathbf{P}$ does not commute with $\mathbf{R}$. Adopting a more compact notation, the partition function of the system represented by Eq. (1) may be written as

$$\begin{aligned}&Z=(2S+1)^N\langle\exp[2\beta J_1(\mathbf{P}+\gamma\mathbf{R}+\alpha\mathbf{Q})]\rangle\,,\\&\gamma=J_2/J_1,\quad\alpha=g\mu H_z/2J_1,\quad\beta=1/kT\,,\end{aligned}\tag{2}$$

where $\langle\mathbf{X}\rangle$ stands for the normalized trace of the $(2S+1)^N$-dimensional direct product matrix representation of the operator $\mathbf{X}$; k is the Boltzmann constant, and T the thermodynamic temperature. The partition function is now expanded as a power series in β in terms of the moments μ_n:

$$\begin{aligned}&Z=(2S+1)^N\sum_{n=0}\frac{(2\beta J_1)^n}{n!}\mu_n\,,\\&\mu_n=\langle(\mathbf{P}+\gamma\mathbf{R}+\alpha\mathbf{Q})^n\rangle\,.\end{aligned}\tag{3}$$

The free energy, equal to $-\beta^{-1}\ln Z$, may likewise be expanded as a power series in β:

$$F=-\beta^{-1}\ln(2S+1)^N-\beta^{-1}\sum_{r=1}\frac{(2\beta J_1)^r}{r!}\lambda_r.\tag{4}$$

The cumulants λ_r may in general be computed from the moments by the use of well-known techniques.[6] In the present context, however, it has been demonstrated in R-W that the cumulants and moments obey a particularly simple relationship:

$$\lambda_r=\Gamma_N\mu_r\,,\tag{5}$$

where the symbol $\Gamma_N f$ means "that part of f which is proportional to N."

The zero-field susceptibility is obtained from the free energy by differentiation:

$$\mathrm{X}=-\left.\frac{\partial^2F}{\partial H^2}\right|_{H=0}=-\left(\frac{g\mu}{2J_1}\right)^2\left.\frac{\partial^2F}{\partial\alpha^2}\right|_{\alpha=0}.\tag{6}$$

This equation shows that only the terms in α^2 are required from the free energy. Since $\mathbf{Q}$ and $\mathbf{P}+\gamma\mathbf{R}$ commute, a binomial expansion of the cumulants or moments is valid

$$\lambda_r=\sum_{t=0}^{r}\frac{r!\alpha^t}{t!(r-t)!}\Gamma_N\langle(\mathbf{P}+\gamma\mathbf{R})^{r-t}\mathbf{Q}^t\rangle.\tag{7}$$

Retaining only the α^2 terms, substitution into Eqs. (4) and (6) yields the susceptibility

$$\mathrm{X}=\beta g^2\mu^2\sum_{r=2}\frac{(2\beta J_1)^{r-2}}{(r-2)!}\Gamma_N\langle(\mathbf{P}+\gamma\mathbf{R})^{r-2}\mathbf{Q}^2\rangle.\tag{8}$$

[4] A. W. Sáenz, Phys. Rev. **119**, 1542 (1960).

[5] Sáenz has, however, provided certain quantities (his $\xi_{i,nr}$) from which the susceptibility could be computed for arbitrary interactions through terms in the third power of the inverse temperature. The remaining operation required is the summation over the interaction constants within the $\xi_{i,nr}$ over the lattice sites; this is equivalent to the diagram counting of R-W or this paper.

[6] R. W. Zwanzig, J. Chem. Phys. **22**, 1420 (1954).

The traces are now expanded in the parameter γ, but because $\mathbf{P}$ and $\mathbf{R}$ do not commute the simple binomial expression does not apply, Instead, it is necessary to write

$$(\mathbf{P}+\gamma\mathbf{R})^{r-2}=\sum_{q=0}^{r-2}\gamma^q\sum_{\text{Perm.}}\mathbf{P}^{r-2-q}\mathbf{R}^q, \tag{9}$$

where $\sum_{\text{Perm.}}$ denotes the sum over all permutations in the order of appearance of the operators $\mathbf{P}$ and $\mathbf{R}$; as an example, for $\mathbf{P}^2\mathbf{R}$, this sum includes $\mathbf{P}^2\mathbf{R}$, $\mathbf{PRP}$, and $\mathbf{RP}^2$. If the above is now substituted into Eq. (8) and the sums are rearranged so that they are symmetrical, the susceptibility can then be written as a double expansion in powers of βJ_1 and βJ_2:

$$\mathrm{X}=\beta g^2\mu^2\sum_{m=0}\sum_{n=0}\frac{(2\beta J_1)^n(2\beta J_2)^m}{(m+n)!}\times\sum_{\text{Perm.}}\Gamma_N\langle\mathbf{P}^n\mathbf{R}^m\mathbf{Q}^2\rangle. \tag{10}$$

As in R-W, the first term of this series ($m=n=0$) is $\Gamma_N\langle\mathbf{Q}^2\rangle=NS(S+1)/3$. Factoring out this term, we obtain the susceptibility in the following final form:

$$\mathrm{X}=(C/T)[1+\sum_{m,n=0}{}'\,a_{nm}(\beta J_1)^n(\beta J_2)^m],$$

$$a_{nm}=\frac{3\times 2^{n+m}}{(n+m)!NS(S+1)}\sum_{\text{Perm.}}\Gamma_N\langle\mathbf{P}^n\mathbf{R}^m\mathbf{Q}^2\rangle, \tag{11}$$

$$C=Ng^2\mu^2S(S+1)/3k,$$

where C is the Curie constant, and where the prime on the summations excludes the term $m=n=0$. The first term of Eq. (11) is Curie's law for noninteracting spins, while succeeding terms represent increasing orders of the statistical mechanical perturbation of the first- and second-neighbor exchange on the free ion paramagnetism. The reciprocal susceptibility may also be expressed as a double expansion

$$\mathrm{X}^{-1}=(T/C)[1+\sum_{m,n=0}{}'\,b_{nm}(\beta J_1)^n(\beta J_2)^m]. \tag{12}$$

The coefficients here may be computed from those of Eq. (11) by the use of the formula,

$$b_{nm}=-\sum_{r=0}^{n}\sum_{q=0}^{m}{}'\,a_{rq}b_{n-r,m-q}. \tag{13}$$

Equations (11) and (12) contain three distinctly different kinds of contributions. The first group of terms are those for which $m=0$; only the first-neighbor interaction appears. The coefficients,

$$a_{n0}=\frac{3\times 2^n}{n!NS(S+1)}\Gamma_N\langle\mathbf{P}^n\mathbf{Q}^2\rangle \tag{14}$$

have already been derived by Rushbrooke and Wood. The first six b_{n0} are in fact tabulated in R-W as functions of S, z, and other lattice parameters such as the $p_n(z)$ (in R-W these are referred to simply as p_n). The $p_n(z)$ further describe the interaction structure, and are defined such that $zNp_n(z)/2(n+2)$ gives the number of $n+2$ sided polygons, which can be placed on the lattice so that the sides form only nearest-neighboring sites.[7]

The next class of terms are those for which $n=0$; only the second-neighbor interaction appears. The coefficients,

$$a_{0m}=\frac{3\times 2^m}{m!NS(S+1)}\Gamma_N\langle\mathbf{R}^m\mathbf{Q}^2\rangle \tag{15}$$

are new but may be trivially obtained from the a_{n0} of R-W. The sole difference between Eqs. (15) and (14) is the appearance of the operator $\mathbf{R}$ in place of $\mathbf{P}$. But the operators $\mathbf{R}$ and $\mathbf{P}$ are entirely similar except that while $\mathbf{P}$ pertains to interactions among first-neighbor pairs, $\mathbf{R}$ describes the interactions between second-neighbor pairs. Therefore, the traces $\langle\mathbf{R}^m\mathbf{Q}^2\rangle$ will be the same as the traces $\langle\mathbf{P}^m\mathbf{Q}^2\rangle$ except that instead of being functions of the first-neighbor lattice parameters z,$p_n(z)$, etc., they will be functions of the second-neighbor lattice parameters y, $p_n(y)$, etc. The $p_n(y)$ are defined such that $yNp_n(y)/2(n+2)$ gives the number of $n+2$ sided polygons which can be placed on the lattice so that the sides join only second-nearest-neighbor sites. Thus, we may write

$$\begin{aligned}a_{0m}(y)&=a_{m0}(z\rightarrow y),\\ b_{0m}(y)&=b_{m0}(z\rightarrow y).\end{aligned} \tag{16}$$

To obtain the numerical values of the $b_{0m}(y)$ for a particular lattice one merely has to take the functions, $b_{m0}(z)$ of R-W and substitute the numerical values of the lattice parameters y, $p_n(y)$, etc., in place of the corresponding z, $p_n(z)$, etc. Values of the $p_n(z)$ for a number of lattices are tabulated in R-W while selected values of the $p_n(z)$ and appropriate $p_n(y)$ are presented in Table I below.

In the final category are those terms for which neither m nor n are zero; both first- and second-neighbor interactions are present. These new terms are not simply related to those already considered and must be computed at length using the diagrammatic technique developed in R-W. The total number that requires detailed calculation, however, is reduced somewhat by a symmetry relation analogous to Eq. (16). Examination of Eq. (11) shows that a_{nm} and a_{mn} differ only be the inter-

[7] The notation, $p_n(z)$ is not meant to imply that $p_n(z)$ is to be considered a function of z; the $p_n(z)$ are only functions of the lattice type under study. The contents of the parenthesis are meant rather to denote the kinds of "bonds" which make up the polygons within the lattice. Thus, the $p_n(z)$ are symbols which describe polygons composed of z type or nearest-neighbor "bonds" only, while the $p_n(y)$ to be introduced later describe polygons composed of y type or second-neighbor "bonds" only, etc.

change of $\mathbf{P}$ and $\mathbf{R}$. Thus, once the traces are taken, a_{nm} and a_{mn} must, as in the case of Eq. (16), be related through the interchange of z and y:

$$a_{mn}(z,y)=a_{nm}(z\rightarrow y, y\rightarrow z),$$
$$b_{mn}(z,y)=b_{nm}(z\rightarrow y, y\rightarrow z). \quad (17)$$

That is, once the function $b_{nm}(z,y)$ is computed, b_{mn} may be obtained from it by the substitution of z for y, and y for z. This procedure will be illustrated in the next section where the details of the calculation of mixed coefficients are described.

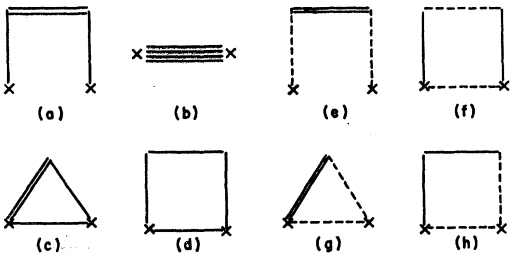

FIG. 1. Selection of typical diagrams encountered in the evaluation of the traces, $\langle \mathbf{P}^4\mathbf{Q}^2\rangle$ and $\Sigma_{\text{Perm.}}\langle \mathbf{P}^2\mathbf{R}^2\mathbf{Q}^2\rangle$.

III. EVALUATION OF THE COEFFICIENTS

The labor of calculating the mixed coefficients is greatly reduced by the use of a diagram technique developed by Rushbrooke and Wood. In R-W, the classification, enumeration, and evaluation of the many different contributions contained in a given $\langle \mathbf{P}^n\mathbf{Q}^2\rangle$ were facilitated by the representation of these contributions in terms of diagrams (localized graphs) on the lattice. The pertinent diagrams consisted of n lines and two crosses. A line connecting nearest-neighboring sites i and j represents the pair exchange operator $\mathbf{S}_i\cdot\mathbf{S}_j$, while a cross on site k represents the spin operator S_{kz}. Several of the diagrams encountered in $\langle \mathbf{P}^4\mathbf{Q}^2\rangle$, for example, are shown in Fig. 1, (a)–(d).

The diagrammatic analysis of the traces $\langle \mathbf{P}^n\mathbf{R}^m\mathbf{Q}^2\rangle$ requires the introduction of another device with which to construct the necessary diagrams. A dashed line connecting next-nearest-neighboring sites k and l will be taken to represent the second-neighbor pair-exchange operator $\mathbf{S}_k\cdot\mathbf{S}_l$. The relevant diagrams then consist of n full lines, m dashed lines, and two crosses. Several of the diagrams derived from $\sum_{\text{Perm.}}\langle \mathbf{P}^2\mathbf{R}^2\mathbf{Q}^2\rangle$, for example are shown in Fig. 1, (e)–(h).

The calculation of the coefficients according to the diagrammatic method involves three separate phases: (a) the finding and cataloging of all the diagrams or graphs which can be constructed from n full lines, m dashed lines, and two crosses, (b) counting the number of times that a diagram can occur on a lattice of N sites, and (c) evaluation of the traces of the products of spin variables which correspond to the diagrams. A significant amount of computation can further be avoided if in addition, at stage (a) one eliminates all those diagrams which will obviously lead to vanishing results. As demonstrated in R-W, the following kinds of diagrams may be completely ignored: all diagrams containing two crosses on the same lattice point (double crosses), all diagrams containing a point with only a single line attached, and all diagrams containing a point with only a single isolated cross attached. Diagrams with double crosses are ignored because an exact cancellation occurs (in order N) between graphs having isolated double crosses and graphs in which the double cross falls on a site with lines attached. The remaining categories provide no contribution since these diagrams represent terms having only a single spin operator associated with a given site; traces of single spin matrixes of course vanish.

In spite of being able to ignore the obviously vanishing diagrams, the number which still have to be considered is not insignificant and increases rapidly with m and n. While certain kinds of graphs which appeared in R-W cannot occur here, there is a far larger number of additional graphs which do enter into the mixed coefficients. For example, diagrams with a high multiplicity of lines such as (b) of Fig. 1 are eliminated from the mixed terms since full lines and dashed lines must not be made to overlap (two sites cannot simultaneously be both first- and second-neighbor pairs). On the other hand, many essentially new diagrams occur because of the possibility of permuting full and dashed lines within a graph of a given geometrical type. As an example consider the square, (d) of Fig. 1 which arose from the trace, $\langle \mathbf{P}^4\mathbf{Q}^2\rangle$ of R-W. In the trace, $\langle \mathbf{P}^2\mathbf{R}^2\mathbf{Q}^2\rangle$, this geometric type is now represented by the two different squares, (f) and (h) of Fig. 1, after the rearrangement of the full and dashed lines within the figure. As a result, a larger number of diagrams appear in a given order of mixed coefficients than are found in the equiva-

TABLE I. Numerical values of the lattice parameters for several crystal structures.

Structure	Face-centered cubic	Body-centered cubic	Simple cubic	Hexagonal close-packed
z	12	8	6	12
y	6	6	12	6
$p_1(z)$	4	0	0	4
$p_1(y)$	0	0	4	0
$p_2(z)$	22	12	4	22
$p_2(y)$	4	4	22	4
$p_1(y;zz)$	4	4	2	4
$p_1(z;yy)$	0	0	0	0
$p_1(y;yz)$	0	0	0	0
$p_1(z;zy)$	4	6	8	4
$p_2(y;zzz)$	24	0	0	24
$p_2(z;yyy)$	0	0	0	0
$p_2(y;zyz)$	16	16	16	14
$p_2(y;zzy)$	8	16	20	10

$a_{31}(z,y) = \frac{4yX^2}{405} \cdot$

	X^2	X	1
z	16	36	24
z^2	-120	-90	
z^3	80		
$p_1(y;zz)$	48	78	27
$zp_1(y;zz)$	-120	-60	
$zp_1(z)$	-40	-20	
$p_2(y;zzz)$	-80	-40	

$a_{13}(z,y) = a_{31}(y,z)$,

$a_{22}(z,y) = \frac{yX^2}{405} \cdot$

	X^2	X	1
z	160	320	180
z^2	-240	-180	
yz	-240	-180	
yz^2	480		
$p_1(y;yz)$	48	78	27
$p_1(y;zz)$	96	156	54
$yp_1(y;zz)$	-480	-240	
$zp_1(y;yz)$	-240	-120	
$p_2(y;zyz)$	-160	-80	
$p_2(y;zzy)$	-160	-80	

FIG. 2. Tabular representation of the coefficients, a_{31}, a_{13}, and a_{22}.

lent order for first neighbors alone. We have therefore restricted our present calculations to coefficients for which $m+n \leqslant 4$.

The enumeration of the occurrences of diagrams on a lattice of N sites is straightforward and has been discussed in R-W and elsewhere.[3,8] In counting the mixed diagrams, however, one has to exercise the additional precaution of distinquishing between diagrams which differ only in the arrangement of full and dashed lines within the figure. Rearrangements among the various lines can lead to distinct diagrams whose occurrence numbers on the lattice will be different. Thus, while (f) and (h) of Fig. 1 are both squares composed of two full and two dashed lines, the number of each on a lattice need not be the same. On a face-centered cubic lattice, for example, the number of occurrences of (f) is twice that of (h).

The final step in the calculation is the evaluation of the traces of the products of spin variables corresponding to the diagrams. At this stage the distinction between full and dashed lines disappears and the evaluation of the traces proceeds exactly according to the scheme outlined in R-W. This circumstance obtains for two reasons. Primarily, both kinds of lines represent operators which have the same scalar product form, $\mathbf{S}_i \cdot \mathbf{S}_k$ (their identity as first- or second-neighbor interactions is only required and completely accounted for in the first stages of the computation described above). Furthermore, the set of distinct terms which correspond to a diagram is precisely the same whether dealing with first neighbors alone or with mixed first- and second-neighbor interactions. This may be seen as follows: First, we observe that any particular diagram, even when its points are labeled (so that it corresponds to a particular set of lattice sites) still represents a number of products of spin matrixes which differ only in the sequence of their factors. Consider diagram (c) of Fig. 1 which derived from $\langle \mathbf{P}^4\mathbf{Q}^2 \rangle$. Labeled clockwise starting with 1 at the top, this diagram represents the traces of all the terms which are the twelve ways of permuting the dot products within the operator $(\mathbf{S}_1 \cdot \mathbf{S}_3)^2 \times (\mathbf{S}_1 \cdot \mathbf{S}_2)(\mathbf{S}_2 \cdot \mathbf{S}_3)\ S_{2z}S_{3z}$. Now, diagram (g) of Fig. 1 (when similarily labeled) represents precisely the same twelve traces. This diagram derives from $\sum_{\text{Perm.}} \langle \mathbf{P}^2\mathbf{R}^2\mathbf{Q}^2 \rangle$ within which we have already included the six different ways of arranging the sequence of $\mathbf{P}$ and $\mathbf{R}$ operators. Each one of these arrangements will then give rise to two distinct permutations with respect to the exchange of positions of the two factors $(\mathbf{S}_1 \cdot \mathbf{S}_2)$ and $(\mathbf{S}_2 \cdot \mathbf{S}_3)$. The twelve traces which result are just those required to give complete correspondence with those of diagram (c). The same considerations are found to apply to all the mixed diagrams encountered in the theory. The various traces for all the diagrams are then evaluated with the aid of a comprehensive list of basic traces given in Appendix 1 of R-W.

The results obtained for the a_{nm} are as follows:

$$a_{11}(z,y) = (8/9)yzX^2 , \tag{18}$$

$$a_{21}(z,y) = (4/27)yX^2\{6z^2X - z[4X+3] - 3p_1(y;zz)[2X+1]\} , \tag{19}$$

$$a_{12}(z,y) = a_{21}(y,z) , \tag{20}$$

where X stands for $S(S+1)$. The coefficients a_{31}, a_{13}, and a_{22} are given in tabular form in Fig. 2. The meaning of the tables is straightforward: The numerical coefficients within the table are multiplied by the power of X above and by the lattice parameters on the left. The sum of all these is then multiplied by the common factor preceding the dot. The numerical values of the lattice parameters for several structures are presented in Table I. The parameters $p_n(z)$ and $p_n(y)$ have been defined above. The other parameters are defined analogously: $p_n(\alpha;\beta\gamma\delta\cdots)$ is the number of $n+2$ sided polygons whose sides are composed of α, β, $\gamma\cdots$ neighbor pairs (in that order) that can be constructed on a specified fixed α neighbor pair within the lattice. The numbers of polygons of type (g), (f), and (h) of Fig. 1 that can be constructed with a specified second-neighbor pair as a base are thus $p_1(y;yz)$, $p_2(y;zyz)$, and $p_2(y;zzy)$, respectively.

The corresponding b_{nm} obtained from Eqs. (18) to (20), Fig. 2, and Eq. (13) are as follows:

$$b_{11} = 0 , \tag{21}$$

$$b_{21} = (4/9)yX^2p_1(y;zz)[2X+1] , \tag{22}$$

$$b_{12} = (4/9)zX^2p_1(z;yy)[2X+1] , \tag{23}$$

while the coefficients b_{31}, b_{13}, and b_{22} are given in tabular form in Fig. 3. Equation (17) has been used to obtain explicit expressions for b_{12} and b_{13} from the derived b_{21} and b_{31}.

[8] P. J. Wojtowicz, Mol. Phys. 6, 157 (1963).

IV. APPLICATION TO GADOLINIUM

This section is concerned with the quality of information which can be obtained from the application of the series expansions to experimental data. We desire to know if it will be possible to extract unambiguous values of the exchange parameters from susceptibility measurements. Our choice of material for such a preliminary test of the theory is ferromagnetic gadolinium metal. This selection was made for several reasons: (i) the Heisenberg model with spin $\frac{7}{2}$ appears to be appropriate for gadolinium, (ii) very good experimental data was available, and (iii) certain interesting questions concerning the exchange interactions in gadolinium have recently been raised by Goodings.[9]

The magnetization[10] and susceptibility[11] data and the spin resonance measurements[12,13] support the view that the magnetism of gadolinium metal arises from the localized $4f^7$ electrons of the gadolinium core. Like Gd^{3+}, the core state appears to be an ${}^8S_{7/2}$ with a well-defined spin of $S=\frac{7}{2}$. On this basis, Goodings[9] has attempted to explain the low-temperature magnetization data under the assumption that the exchange interactions are of the nearest-neighbor Heisenberg type. Using a highly detailed spin-wave analysis Goodings has succeeded in obtaining an excellent fit to the magnetization from absolute zero to about 0.8 T_c; the value of the nearest-neighbor exchange parameter required is $J_1/k=2.1$°K. Applying the Rushbrooke and Wood[2] formula for the Curie point (also derived from the nearest-neighbor Heisenberg model) to gadolinium, however, yielded a different value for the exchange: $J_1/k=2.9$°K. Goodings has attributed this discrepancy to the neglect of the second- and higher order neighbor interactions in both theories. He has further concluded, on the basis of qualitative arguments, that interactions through at least fifth neighbors are significant in gadolinium, and that the interactions beyond first neighbors are on the average more antiferromagnetic than ferromagnetic.

The high-temperature susceptibility data used in the present study was kindly supplied to us by Dr. Sigurds Arajs of the United States Steel Research Center. These data are qualitatively similar to that previously published by Arajs and Colvin.[11] The new measurements have been made on a more pure sample and the results are more precise with much less scatter. The anomaly at 750°K was also much smaller for this sample but was still sufficiently large to preclude the extension of our analysis above 750°K. The temperature range examined fell between 375 and 743°K; the Curie point is about 293°K.

The first step in the analysis was the estimation and

$b_{31}=\frac{4yX^2}{405}\cdot$

	X^2	X	1
$p_1(y;zz)$	-48	-78	-27
$p_2(y;zzz)$	80	40	

$b_{13}=\frac{4zX^2}{405}\cdot$

	X^2	X	1
$p_1(z;yy)$	-48	-78	-27
$p_2(z;yyy)$	80	40	

$b_{22}=\frac{yX^2}{405}\cdot$

	X^2	X	1
z		-80	-90
$p_1(y;yz)$	-48	-78	-27
$p_1(y;zz)$	-96	-156	-54
$p_2(y;zyz)$	160	80	
$p_2(y;zzy)$	160	80	

FIG. 3. Tabular representation of the coefficients, b_{31}, b_{13}, and b_{22}.

subtraction of the temperature-independent susceptibility which arises from the atomic core diamagnetism and the conduction electron paramagnetism. The linear extrapolation of the high-temperature data on a X versus $(T-\theta)^{-1}$ plot (θ is an approximate extrapolated paramagnetic Curie point, here 300–310°K) gave a temperature-independent contribution of 4.1×10^{-6} cm^3/g. This component amounts to 0.25% and 3.5% of thes pin susceptibility at 375 and 743°K, respectively.

The remaining spin susceptibility was analyzed with the aid of Eq. (12). For the hexagonal close-packed lattice with $S=\frac{7}{2}$ the numerical values of the coefficients used are

$$\begin{aligned}
&b_{10}=-126 && b_{20}=1\,386\\
&b_{30}=50\,946 && b_{40}=2\,456\,280.75\\
&b_{50}=137\,048\,223.45 && b_{60}=8\,230\,853\,289\\
&b_{01}=-63 && b_{02}=693\\
&b_{03}=-3192 && b_{04}=275\,580.375\\
&b_{11}=0 && b_{21}=85\,995\\
&b_{12}=0 && b_{31}=6\,449\,625\\
&b_{22}=3165\,277.5 && b_{13}=0.
\end{aligned} \tag{24}$$

The procedure adopted for the determination of the exchange constants is as follows: values of J_1 and J_2 were assumed and substituted into Eq. (12). The theory and the data were fitted by adjusting the Curie constant C so as to give the least root-mean-square deviation (rmsd). The resulting rmsd for each pair of exchange constants were plotted as a function of J_1 and J_2. The pair of interaction constants which give the best fit to the data are then determined by seeking the position of the absolute minimum in the surface, rmsd of J_1 and J_2.

The anticipated sharp and well-defined minimum was not found, however. Instead, the surface, rmsd of J_1 and J_2 displayed an almost linear deep trough. Though quite deep and narrow, the trough, unfortunately, had only a very shallow minimum along its length. Thus, all pairs J_1, J_2 along the bottom of the trough give almost equally good fits to the data; rather than being able to

[9] D. A. Goodings, Phys. Rev. **127**, 1532 (1962).
[10] J. F. Elliot, S. Legvold, and F. H. Spedding, Phys. Rev. **91**, 28 (1953).
[11] S. Arajs and R. V. Colvin, J. Appl. Phys. **32**, 336 S (1961).
[12] A. F. Kip, Rev. Mod. Phys. **25**, 229 (1953).
[13] J. Popplewell and R. S. Tebble, J. Appl. Phys. **34**, 1343 (1963).

specify a unique set of exchange constants, all that is possible is the determination of one relation between J_1 and J_2. This relationship will be given by the equation of the projection of the trough bottom onto the J_1, J_2 plane. We believe that this will be a general feature to be encountered in all applications of the present theory to experimental susceptibilities.[14] In order to obtain unambiguous values of the interaction parameters it appears necessary to analyze additional experimental data. This can be the spin-wave analysis of low-temperature properties, the series expansion analysis of the high-temperature heat capacity[15] or the Green's function analysis of the Curie point[16] (all based on 1st and 2nd-neighbor interactions, of course).

In the present example the equation of the projection of the trough bottom onto the J_1, J_2 plane is

$$(J_1/k)+0.621(J_2/k)-0.030(J_2/k)^2=2.807\,, \quad (25)$$

$$-0.50\leqslant(J_2/k)\leqslant 1.00, \quad 3.12\geqslant(J_1/k)\geqslant 2.22\,. \quad (26)$$

All pairs J_1, J_2 which satisfy Eqs. (25) and (26) give almost the same rmsd. At $J_2/k=-0.50$, the rmsd is 24.1 g/cm^3, while at $J_2/k=1.00$, the rmsd is 23.8 g/cm^3 (these correspond to average deviations of about $\frac{1}{2}\%$). There is a shallow minimum along the trough at $J_1/k=2.73$, $J_2/k=0.13$ where the rmsd is 22.1 g/cm^3; beyond the limits of Eq. (26) the rmsd rises rapidly and the trough disappears.

For all values of J_1 and J_2 satisfying Eqs. (25) and (26) the least-squares determined Curie constant assumed the same value. On a molar basis the value obtained was 7.41 which corresponds to $g=1.94$. This is in very close agreement with the $g=1.96\pm0.03$ obtained from paramagnetic resonance.[13]

We have made a preliminary attempt at specifying the individual values of J_1 and J_2 in gadolinium by using the Tahir-Kheli and Jarrett[16] Green's function analysis of the Curie point. Though these results pertain explicitly to the face-centered cubic lattice (with $S=\frac{7}{2}$), they should be quite accurate for hexagonal close-packed gadolinium as well (compare the similarity in structure parameters for fcc and hcp in Table I and in R-W). Now, because this is a two-parameter theory describing one experimental point, it can provide but one relationship between J_1 and J_2. Substituting the measured value,[10] $T_c=289$°K, the following equation is obtained:

$$J_1/k+0.64J_2/k=2.90\,. \quad (27)$$

Notice that Eqs. (25) and (27) are almost identical, giving very nearly the same line in that portion of the J_1, J_2 plane in or near the limits of Eq. (26).

Two interpretations of this occurrence are possible. First, one may assume that the information obtained from the two treatments is essentially the same, the small deviations between Eqs. (25) and (27) being attributed to the different mathematical approximations involved. The near coincidence of the two results may then be cited as evidence for the equivalence of these two widely differing forms of approximation to the statistical thermodynamics of the first- and second-neighbor Heisenberg model. On the other hand, one could assume that the two theories provide essentially independent information. In that case, the intersection of the curves, Eqs. (25) and (27), could then be considered to give the best values of J_1 and J_2. The intersection occurs at $J_1/k=2.0$, $J_2/k=1.4$; too much confidence should not be placed on these values since the intersection of the two almost parallel curves is highly sensitive to small displacements in either or both of Eqs. (25) and (27). It is of interest to note, however, that the intersection quoted suggests a definitely positive value for J_2 in contrast to the conclusion of Goodings.[9] At the present time we believe that the first interpretation of these results is the more probable.

ACKNOWLEDGMENT

The authors wish to express their sincere appreciation to Dr. Sigurds Arajs of the United States Steel Research Center for kindly supplying the experimental data on the susceptibility of gadolinium metal.

[14] We have in fact observed this behavior in the preliminary analysis of the susceptibilities of the europous chalcogenides. The same results are to be expected in other examples as well since all inverse susceptibility data are qualitatively quite similar in appearance.

[15] P. J. Wojtowicz, J. Appl. Phys. **35**, 991 (1964).

[16] R. A. Tahir-Kheli and H. S. Jarrett, Bull. Am. Phys. Soc. **9**, 463 (1964).